

# Irradiation tests for $U_3Si$ –Al dispersion fuels with aluminum cladding

H.T. Chae \*, H. Kim, C.S. Lee, B.J. Jun, J.M. Park, C.K. Kim, D.S. Sohn

*Korea Atomic Energy Research Institute P.O. Box 105, Yuseong, Daejeon 305-600, Republic of Korea*

Received 29 July 2006; accepted 18 March 2007

## Abstract

The HANARO fuel element is made of a cylindrical fuel meat, top and bottom aluminum end plugs and an aluminum cladding with eight longitudinal fins. The fuel meat of each fuel element consists of a dispersion of small particles of a high density uranium silicide ( $U_3Si$ ) compound in a continuous aluminum matrix. To verify the irradiation performance of the HANARO fuel at a high power and a high burnup, in-pile irradiation tests were performed in the HANARO core. Detailed non-destructive and destructive post-irradiation examinations were conducted. It was verified through the irradiation tests that the HANARO fuel maintains a proper in-pile performance and integrity even at a high power of 121 kW/m and up to a high burnup of 85 at.% U-235.

© 2007 Elsevier B.V. All rights reserved.

PACS: 28.50

## 1. Introduction

HANARO is a light-water-cooled and heavy-water-reflected research reactor designed and operated as summarized in Table 1. The hybrid-type core is composed of an inner and an outer core as shown in Fig. 1. The inner core, with a 0.47 m effective diameter and 1.2 m in height, has 23 hexagonal and 8 circular flow channels. Each hexagonal flow channel, formed by a hexagonal flow tube, is loaded with a hexagonal fuel bundle which has 36 fuel elements. The circular flow channel formed by a circular flow tube is loaded with a circular fuel bundle which has 18 fuel elements. The compact core results in a high power density and high neutron flux.

Wood [1] reported the development process of the LEU (low enrichment uranium) fuels for Canadian research reactor. They had developed and tested the fuel rods of uranium silicide dispersed in aluminum and clad in alumi-

num. Irradiation performances of the  $U_3Si$  fuels were verified by the core conversion of HEU (high enrichment uranium) to LEU fuels of NRU reactor in Canada [2] and the succeeding testing and PIEs (Post-Irradiation Examination) [3]. AECL (Atomic Energy Canada Limited) manufactured Al–61 wt%  $U_3Si$  fuel for the NRU and the HANARO reactors.

When the reactor operating license was issued for HANARO in 1995, the limitation for its rated power was imposed by the regulatory body, KINS (Korea Institute of Nuclear Safety). KINS required KAERI (Korea Atomic Energy Research Institute) to obtain more fuel performance data at a higher linear power rate which would prove fuel integrity [4]. To verify the irradiation performance of the HANARO fuel at a high power and high burnup, in-pile irradiation tests were performed by using several test bundles. Detailed non-destructive and destructive PIEs, such as the measurement of the burnup distribution, fuel swelling, clad corrosion, dimensional changes, fuel rod bending strength, micro-structure, etc., were conducted in the IMEF (Irradiated Material Examination Facility) located inside the HANARO boundary. The

\* Corresponding author. Tel.: +82 42 868 8620; fax : +82 42 868 8341.  
E-mail address: [htchae@kaeri.re.kr](mailto:htchae@kaeri.re.kr) (H.T. Chae).

Table 1  
Design characteristics of the HANARO

Items	Design data	Items	Design data
Reactor type	Open-tank-in-pool	Absorber	Hafnium
Power	30 MW <sub>th</sub>	Core cooling	Upward forced convection
Fuel meat	19.75 wt% U-235, U <sub>3</sub> Si dispersion fuel in Al matrix	Core inlet/outlet temperature	35/45 °C
Cladding	Co-extruded aluminum alloy AA-1060 (99.60% min. Al) with 8 fins	Core inlet/outlet pressure	0.409/0.2 MPa
Fuel assembly	36-element hexagonal assembly/18-element circular assembly	Core flow velocity	7.3 m/sec
Coolant	H <sub>2</sub> O	Max. linear power	0.0953 MW/m
Moderator	H <sub>2</sub> O/D <sub>2</sub> O	Average discharge burnup	>50 at.% U-235
Reflector	D <sub>2</sub> O	Core residence time	175 full power days

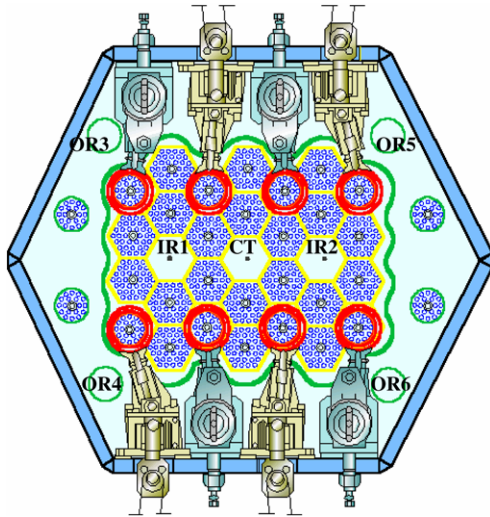


Fig. 1. Cross section of HANARO core.

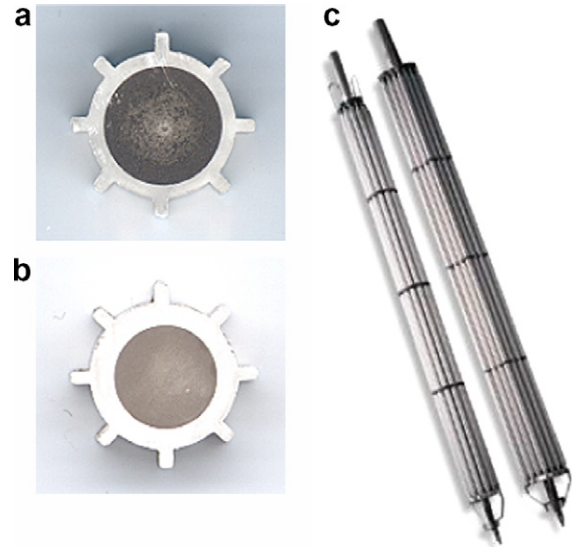


Fig. 2. Cross section of fuel elements and fuel assemblies. (a) Standard fuel element. (b) Reduced fuel element. (c) Circular and hexagonal fuel assemblies.

measured results were analyzed and compared with the design criteria of the HANARO fuel.

## 2. HANARO fuel

### 2.1. Fuel element

The HANARO fuel element is made of a cylindrical fuel meat, top and bottom aluminum end plugs and an aluminum cladding with eight longitudinal fins. The fuel elements are divided into the standard one with  $\phi$  6.35 mm meat diameter and the reduced one with  $\phi$  5.49 mm meat diameter as shown in Fig. 2. The fuel meat of each fuel element consists of a dispersion of small particles of a high density uranium silicide (U<sub>3</sub>Si) compound, in a continuous aluminum matrix. The driver fuel contains low-enriched uranium (less than 20 wt% U-235 in total uranium) in a U<sub>3</sub>Si inter-metallic compound dispersed in aluminum. An aluminum alloy, AA-1060 (99.60% min. Al) is used as a cladding material.

### 2.2. Fuel design requirements

The fundamental fuel design requirements of an adequate fissile content, heat transfer capability, strength

and dimensional stability should be met through the design and safety analyses. The design limits for a normal operation are for margin of the onset of nucleate boiling ( $\Delta T_{ONB}$ ), fuel temperature, and temperature drop across the aluminum oxide layer. The safety limits for anticipated occurrences and accident conditions are the minimum critical heat flux ratio and the maximum fuel temperature. Also the amount of swelling of the fuel meat shall not be greater than 20 vol.%.

### 2.3. Licensing issues

For the verification of the fuel performance in the design stage of HANARO, KAERI relied on the AECL's experimental data. However, the maximum linear heat generation rate from the fuel element in the equilibrium core conditions was quite close to the maximum value which had been experienced in the AECL's mini element irradiation tests. Thus KINS imposed a limitation for HANARO's rated power when the reactor operating license was issued. KINS required KAERI to obtain more experimental data at a higher linear heat rate which would prove the fuel integrity.

### 3. Irradiation tests

#### 3.1. Type-A tests [5]

To verify the irradiation performance of the HANARO fuel at a high power and burnup, in-pile irradiation tests were performed. Two un-instrumented test fuel called Type-A bundles (KFH-051 and KFH-067) for a higher burnup irradiation were designed by KAERI and fabricated by AECL. The test fuel bundles were made of six fuel elements located in the outer ring of the hexagonal fuel assembly and 30 aluminum dummy elements as shown in Fig. 3. The test fuel bundles were irradiated for 206 reactor operation days (KFH-051) and 293 reactor operation days (KFH-067) in the HANARO core. The irradiation test conditions were summarized in Table 2. Type-A fuel bundles were discharged after a 69.9 at.% U-235 average and a 85.5 at.% U-235 peak burnup, respectively.

#### 3.2. High power irradiation test [6]

Another hexagonal test fuel bundle (KH99H-001) for the high power irradiation test was developed along with the localization plan for self-manufacturing of the HANA-

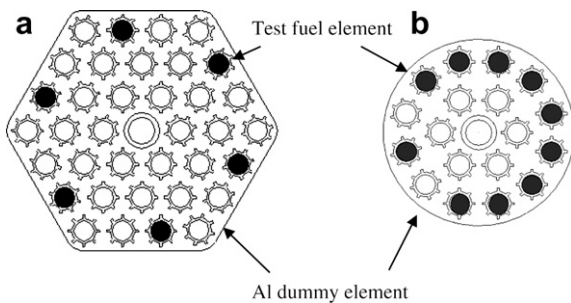


Fig. 3. Cross section of the irradiation test bundles. (a) Hexagonal test bundle. (b) Circular test bundle.

RO fuel in KAERI. The high power test fuel bundle was composed of six fuel and 30 dummy elements as illustrated in Fig. 3. The six fuel elements consisted of three pulverized and three atomized U<sub>3</sub>Si fuels. The test assembly was irradiated for 173.7 reactor operation days in the central thimble(CT) hole with the highest neutron flux in the HANARO core. The reactor physics calculations showed an average discharge burnup of 63 at.% U-235, a maximum local burnup of 77 at.% U-235, an average linear power of 83 kW/m and a maximum linear power of 121.6 kW/m as shown in Fig. 4.

#### 3.3. KOMO-2 irradiation test [7]

As the 2nd irradiation test for the U–Mo fuel, the circular test fuel assembly consisting of 10 test fuel rods as shown in Fig. 1 was loaded into the HANARO core for one year up to an average burnup of 60.8 at.% U-235. Only the surface corrosion data of the KOMO-2 results were used in this paper due to the different fuel composition. One surface treated fuel with a pre-oxidation among the

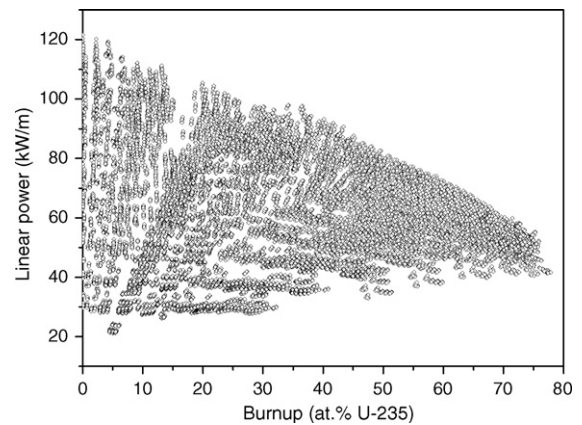


Fig. 4. Linear power distributions of the high power irradiation test bundle.

Table 2  
Irradiation test conditions in the HANARO

Items	U <sub>3</sub> Si fuel tests	U–Mo fuel test		
Fuel identification	KFH-051 (Type-A)	KFH-067 (Type-A)	KH99H-001 (High power)	KOMO-2
Test fuel assembly	Hexagonal assembly with 6 test rods			Circular assembly with 10 test rods
Uranium density, kg U/m <sup>3</sup>	3.15E-3			4.0E-3 or 4.5E-3
Fuel meat size, m	ϕ 6.35E-3 dia., 0.7 length			ϕ 6.35E-3 or 5.49E-3 dia., 0.21 or 0.31 length
Irradiation hole in HANARO	IR2	IR1	CT	OR5
Max. linear power, MW/m	0.0878	0.0962	0.1216	0.112
Fuel surface heat flux, MW/m <sup>2</sup>	1.2–3.5	1.2–3.5	1.5–4.5	1.5–4.5
Fuel surface temperature, °C	45–90	45–90	50–110	50–110
Coolant temperature, °C	30–40	30–40	30–45	30–45
Coolant water, pH	5.5–5.7	5.5–5.7	5.5–5.7	5.5–5.7
Reactor power, MW	15, 20, 22	15, 20, 22	20, 22, 24	24
Reactor operation days	206	293	173	177
Average/maximum discharge burnup, at.% U-235	52.8/69.9	69.7/85.5	63/77	60.8/71.2

test rods was included to investigate the reduction possibility of surface corrosion.

#### 4. Post-irradiation examination

##### 4.1. Visual inspection

In the service pool of the HANARO, an under-water visual inspection system was deployed. Periodical examinations showed a good condition for the mechanical integrity of the test fuel bundles. One of the special findings was that some dark discolorations appeared at the location of the fuel which experienced a relatively high heat flux. In the hot cell examination, it was confirmed that the dark dis-

colorations in the under-water conditions were the white ones in the air conditions. And through the metallography of the irradiation sample, the above discolorations are thought to be attributable to a kind of aluminum oxide layer caused by a local overheating.

##### 4.2. Swelling

Uranium silicide dispersion fuels in aluminum swell due to irradiation. In the case of HANARO, a limit of 20% volumetric swelling had been set. Swelling had been conservatively estimated to be less than 1 vol.% per 10 at.% U-235 burnup at a terminal burnup in the AECL performance tests [8]. The meat diameter changes were measured from

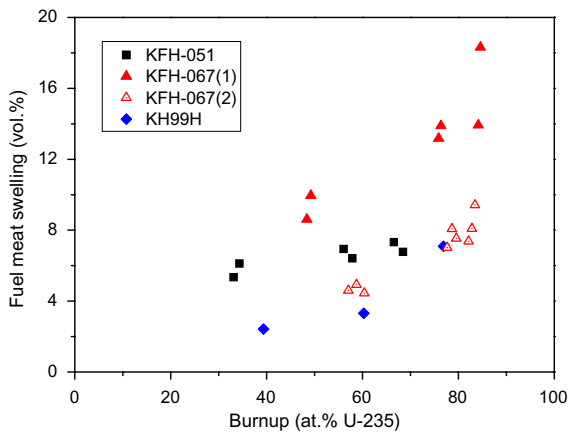


Fig. 5. Volumetric swelling measured by the immersion density method.

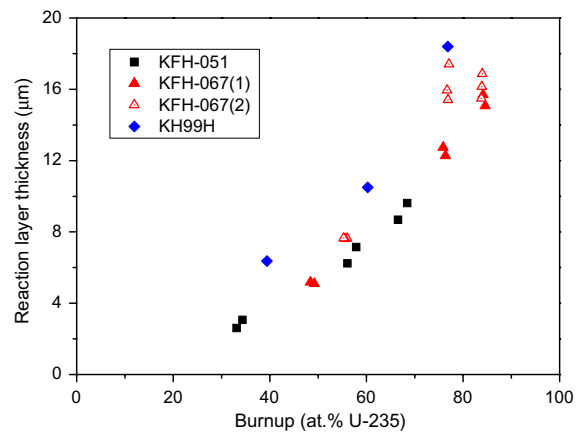


Fig. 7. Reaction layer thickness of the fuel particle.

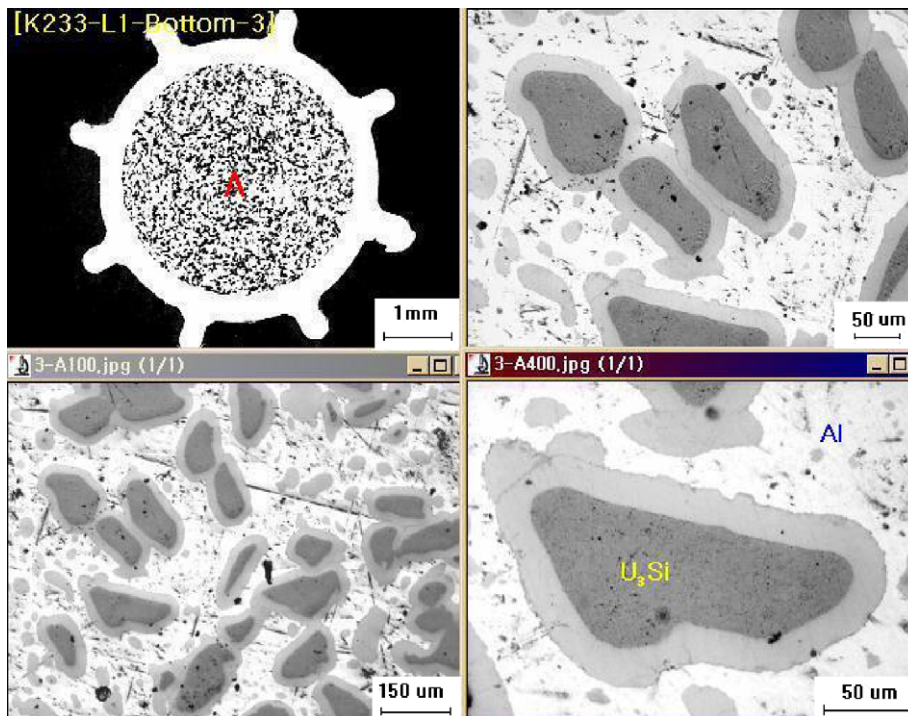


Fig. 6. Micrographs of the fuel particles and reaction layers.



the micrographs by averaging several circumferential data or the cross-sectional area of the meat. But we could not confirm that the cut-off surface was perfectly perpendicular to the axis of the fuel rod. Therefore we preferred immersion density measurements over diameter measurements for the volume change assessment of the fuel meat. Fig. 5 shows the irradiation swellings with an increase of the burnup for the fuel meat specimens in which the cladding was removed. Maximum swelling reached to about 18 vol.% in the KFH-067(1) sample. Thus we enlarged the sample size by increasing the specimen's length from 3 mm to 10 mm since the larger volume mitigates the linearly un-even distribution of uranium. These samples denoted by KFH-067(2)

in Fig. 5 showed a good swelling performance; lower than 10 vol.% at the highest burnup.

### 4.3. Reaction layer

The micrographs of the fuel meats revealed that a chemical reaction forming uranium-aluminide compound ( $UAl_3$  or  $UAl_3Si_{1/3}$ ) of a lower density had occurred between the fuel particles and aluminum matrix as shown in Fig. 6. These reaction layers surrounding the uranium particles become one of the main causes of the fuel swelling. The reaction product was mainly confined to the peripheral regions of the fuel particles and was typically 5  $\mu m$  thick

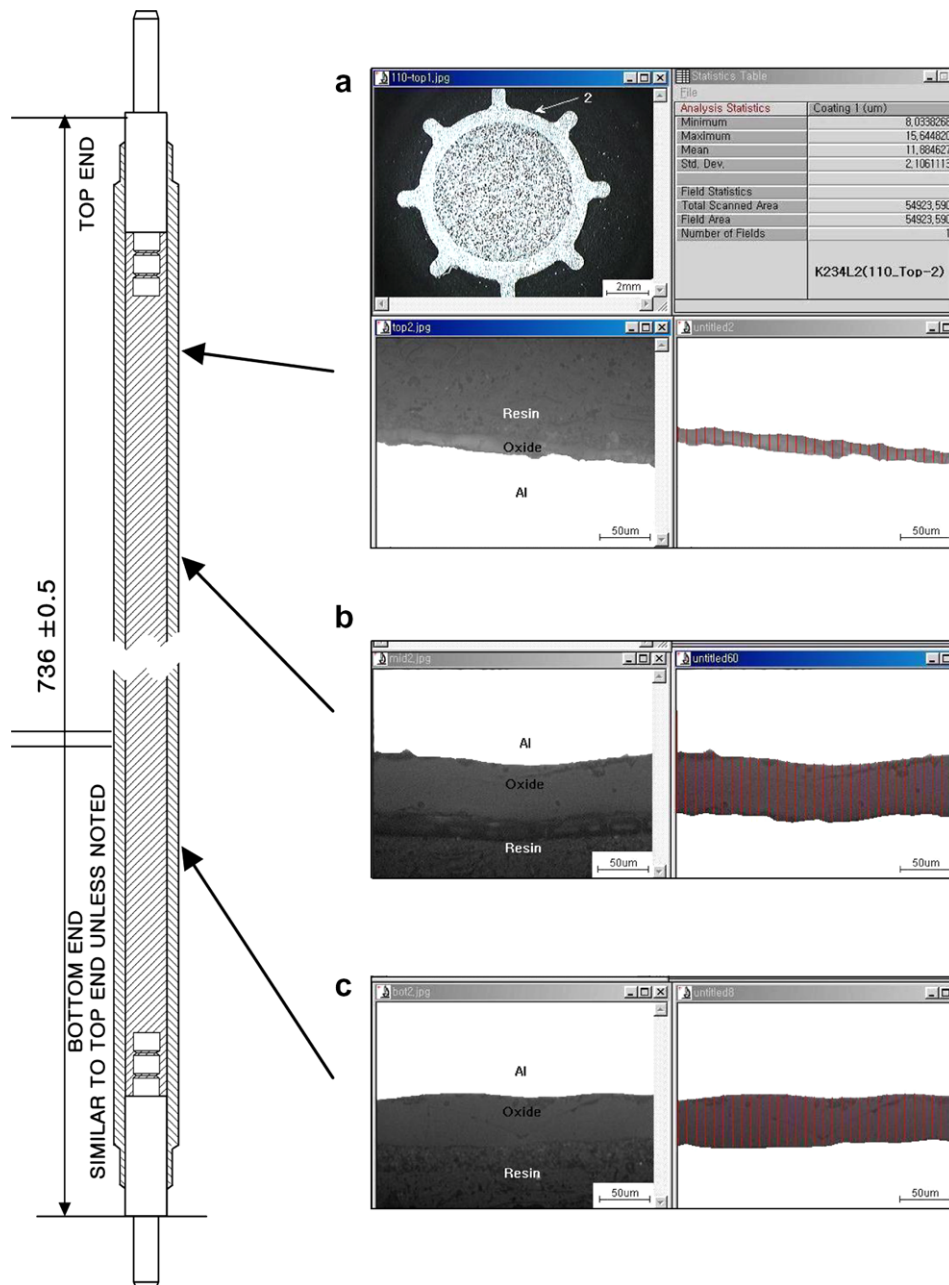


Fig. 8. Horizontal cutting views of the oxide layers on fuel surface: (a) 142 mm from top end, (b) 292 mm from top end, (c) 542 mm from top end.

after a 40 at.% U-235 burnup and 20  $\mu\text{m}$  thick after an 80 at.% U-235 burnup as Fig. 7. A small amount of porosity was noted at the edges of some of the fuel particles.

#### 4.4. Corrosion behavior

##### 4.4.1. Corrosion characteristics

The growth of the corrosion layer ( $\text{Al}_2\text{O}_3 \cdot \text{H}_2\text{O}$ ) on the aluminum cladding surface is influenced by such variables as the temperatures of the cladding and the coolant, the coolant chemistry, the surface heat flux and the corrosion layer thickness. Effect of the corrosion of the aluminum alloy cladding upon the fuel performance is a temperature increase of the fuel and cladding due to a very low thermal conductivity of the aluminum oxide, which can lead to a loss of the creep resistance of the cladding and the thermal expansion of the fuel, and the fuel failure by a perforation of the cladding due to an excessive corrosion. As the corrosion layer of the aluminum cladding increases above a certain limit, a spallation of the corrosion layer can occur. As a design limit of the cladding oxidation, an oxide spallation was conservatively selected even though it does not directly result in a fuel failure.

##### 4.4.2. Oxide layer thickness

An oxide thickness survey was done by using each metallographic sample as illustrated in Fig. 8. Thicker oxides were created on the surfaces of the test fuel elements that had been operated at high heat ratings or high burnups. The range of the oxide layers were typically from 10 to 80  $\mu\text{m}$  along with the burnup as shown in Fig. 9. The reactor operating conditions including the fuel surface temperatures during the irradiation tests were summarized in Table 2. We obtained the following correlation between the burnup and the oxide layer thickness by the regression method. The distribution of the predicted ones with a standard deviation of 13.57 is revealed in Fig. 10 and the application ranges of the correlation are given in Table 2;

$$X_{\text{OX}} = 0.0049(\text{BU})^{2.1063} \quad (1)$$

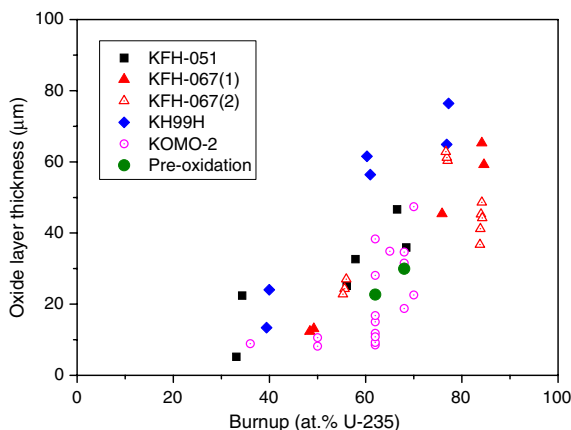


Fig. 9. Oxide layer thickness of the fuel cladding surface.

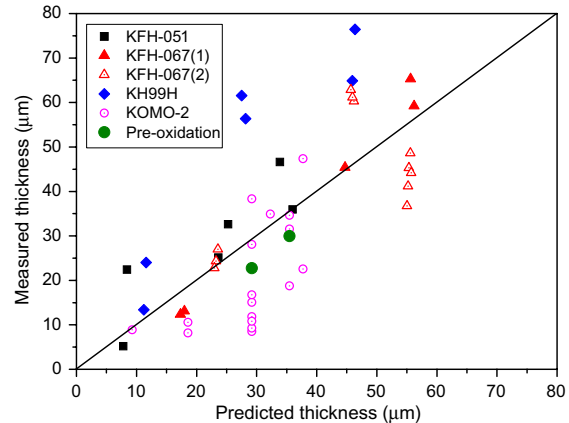


Fig. 10. Comparison of measured and predicted oxide layer thickness.

where  $X_{\text{OX}}$  = oxide layer thickness ( $\mu\text{m}$ )

BU = burnup(at.% U-235).

It was confirmed in the ANS (advanced neutron source) corrosion test that the oxide film growth is strongly dependent on the coolant water chemistry, and that a particularly sensitive increase is seen in the range of pH 4.9–5.1 [9]. Considering that the core coolant is controlled at pH 5.6 in HANARO, the thicker oxide layers than the expected ones seem to be caused by the water chemistry. We could not find any evidence of a spallation of the oxide layer from the micrographs. It was confirmed in the HFIR experiment that the oxide spallation is followed by a severe deformation of the aluminum surface and an extensive sub-surface voiding. Even though such damage may reduce the effective thermal conductance of the clad, the intact aluminum cladding over 90% of the original thickness maintained the cladding integrity as shown in Fig. 8. Thus the thick oxide layers appear to have no detrimental effect on the fuel element performance of the HANARO fuel.

##### 4.4.3. Pre-oxidation of cladding surface

Pre-oxidation test rod had been exposed to a water vapor atmosphere at elevated temperature before it was loaded into the core. The autoclave was used to drive a hard oxide film at the cladding surface with the temperature of 180  $^{\circ}\text{C}$  and the vapor pressure of 1.03 MPa for 16 h. The pre-oxidation fuel rod showed a sound surface appearance with the film thickness of about 3–5  $\mu\text{m}$ . But the irradiation test showed that the thin-layered pre-oxidation treatment is not effective in reducing the oxidation rate at the cladding surface because the fuel rods without pre-oxidation exhibited also similar oxide thickness in Fig. 9.

## 5. Conclusions

The irradiation tests using the HANARO fuels were performed to verify the irradiation performance at a high power and burnup. The three hexagonal test fuel bundles and the one circular test fuel bundle were used. The maximum discharged burnup and linear power were

69.9 at.% U-235 average and 85.5 at.% U-235 peak with an 83 kW/m average and 121.6 kW/m peak, respectively. Through detailed non-destructive and destructive PIE, we could find that some discolorations observed on the fuel surface were related to a kind of aluminum oxide layer caused by a local overheating. Swelling data obtained from the thicker samples by the immersion density method was lower than 10 vol.% at a terminal burnup. The thicker oxide layer than the expected one in the design stage appeared to be due to the water chemistry. But the thick oxides do not threaten the cladding integrity because there was no indication of a spallation in the micrographs of the oxide layers. In conclusion, it was verified that the HANA-RO fuel maintains a proper in-pile performance and integrity even at a high power of 121 kW/m and up to a high burnup of 85 at.% U-235.

## References

- [1] J.C. Wood, M.T. Foo, L.C. Berthiaume, in: Proceedings of the International Meeting on Research and Test Reactor Core Conversions from HEU to LEU Fuels, Argonne, Illinois, USA, 1982.
- [2] D.F. Sears, M.D. Atfield, I.C. Kennedy, The Conversion of NRU from HEU to LEU Fuel, IAEA-SM-310/73, 1990.
- [3] D.F. Sears, N. Wang, in: Proceedings of the International Meeting on Reduced Enrichment for Research and Test Reactors, Wyoming, USA, October 1997.
- [4] G.Y. Han, I.C. Lim, H.T. Chae, D.S. Sohn, J.B. Lee, in: Proceedings of the International Groups on Research Reactor Meeting, Daejeon, Korea, 1998.
- [5] H.T. Chae, C.S. Lee, I.C. Lim, H. Kim, B.J. Jun, H.R. Kim, J.M. Park, C.K. Kim, C.B. Lee, B.G. Kim, D.S. Sohn, in: Proceedings of the International Meeting on Reduced Enrichment for Research and Test Reactors, Vienna, Austria, November 2004.
- [6] K.H. Kim, J.M. Park, B.O. Yoo, D.K. Park, C.S. Lee, C.K. Kim, in: Proceedings of the Korean Nuclear Society Autumn Meeting, Yon-gyeong, Korea, October 2002.
- [7] C.K. Kim, H.J. Ryu, S.J. Oh, K.H. Kim, J.M. Park, Y.S. Choo, D.G. Park, H.T. Chae, C.S. Lee, D.S. Sohn, in: Proceedings of the International Meeting on Reduced Enrichment for Research and Test Reactors, Vienna, Austria, November 2004.
- [8] D.F. Sears, M.F. Primeau, C. Buchanan, D. Rose, in: Proceedings of the International Meeting on Reduced Enrichment for Research and Test Reactors, Virginia, USA, September 1994.
- [9] D.L. Selby, R.M. Harrington, P.B. Thomson, Advanced Neutron Source (ANS) Project Progress Report FY 1994, ORNL-6821, Oak Ridge National Laboratory, January 1995.